Neuroergonomics and Cognitive Engineering, Vol. 167, 2025, 137–147
https://doi.org/10.54941/ahfe1006135

Exploratory Study on EEG Characteristics of Visual Vestibular Conflict Induced Motion Sickness

Chen Xinjia[1] and Wei Yue[1,2]

[1]Department of Basic Psychology, School of Psychology, Shenzhen University, 3688 Nanhai Avenue, Nanshan District, Shenzhen 518060, China
[2]HKUST-Shenzhen Research Institute, 9 Yuexing First Road, South Area, Hi-tech Park, Nanshan, Shenzhen 518057, China

ABSTRACT

Motion sickness, commonly introduced by conflicting visual-vestibular inputs, remains inadequately characterized at the neurophysiological level, with limited quantitative biomarkers for sensory conflict detection. This study investigated electroencephalographic (EEG) activity patterns associated with varying degrees of visual-vestibular congruence to identify potential neural correlates of sensory conflict. Six healthy participants (aged 18–22 years) underwent controlled motion stimuli while EEG data were recorded using a wireless system. Participants were seated in an electrically powered wheelchair traversing a 3-meter linear track under three experimental conditions: (1) congruent visual-vestibular stimuli, (2) vestibular stimulation without visual input, and (3) conflicting visual-vestibular information. Both forward and backward motion were explored. Spectral analysis of EEG data revealed condition-dependent variations in neural oscillations. Notably, delta-band (1–4 Hz) power demonstrated the highest magnitude during visual-vestibular conflict and the lowest during congruent stimulation. Direction-specific effects were observed, with significant differences in delta and alpha band power between forward and backward motion, particularly in the central (Cz) and right occipital (O2) regions. These findings suggest that EEG spectral signatures may serve as objective indicators of sensory conflict during motion, potentially informing early detection strategies and therapeutic interventions for motion sickness.

Keywords: Visual signal, Sensory conflict, Motion sickness, EEG

INTRODUCTION

Motion sickness refers to a syndrome characterized by vestibular and autonomic nervous responses, such as nausea, vomiting, dizziness, and other discomforts, experienced in certain motion environments, such as when people travel in enclosed vehicles like cars and airplanes, or when immersed in 3D virtual reality environments (Tian et al., 2022; Wei et al., 2024). The exact mechanisms behind motion sickness remain unclear. Several theories have been proposed, including the sensory conflict theory, vestibular hypersensitivity theory, and the postural instability theory. Among them, the sensory conflict theory is the most widely accepted, with both animal

© 2025. Published by AHFE Open Access. All rights reserved.

and human studies confirming the critical role of the vestibular system in the development of motion sickness (Fetsch et al., 2011; Koch et al., 2018; Lackner, 2014; Schmäl, 2013; Wei et al., 2024). This theory, initially proposed by Reason and Brand, suggests that the mismatch between actual sensory input and the sensory information integrated into the "internal model" formed by prior experiences can lead to motion sickness (Parker, 1977; Reason & Brand, 1975). According to the sensory conflict theory, the new "internal model" can be generated by neural storage of previously experienced motion patterns, and the existing "internal model" may be offset by new models created after repeated exposure to motion (Zhang et al., 2016). The vestibular system regulates cardiovascular function during motion and posture changes via vestibular-sympathetic reflexes (Yates et al., 2014). Research shows that brain regions associated with nausea and vomiting not only receive vestibular signals but also gastrointestinal signals, suggesting that visceral mechanosensory information may be involved in the vestibular-autonomic response during motion sickness (Yates et al., 2014).

Motion sickness susceptibility exhibits significant individual differences, with age being a prominent factor. The incidence of motion sickness is low in infants, typically starting around 6–7 years of age, peaking at 9 years old (Henriques et al., 2014). The primary tool for studying motion sickness susceptibility is the Motion Sickness Susceptibility Questionnaire (MSSQ-short, Golding, 1998), and motion sickness severity is measured using subjective assessment methods, including the Motion Sickness Questionnaire (MSQ) and its various modified versions. Among them, the Simulator Sickness Questionnaire (SSQ), proposed by Kennedy, is the most commonly used by researchers (Jang et al., 2022). Jang et al., (2022) analyzed the relationship between EEG signals and SSQ, finding that delta waves significantly increased and alpha waves significantly decreased compared to baseline conditions.

Research on cortical regions involved in self-motion perception has identified several key areas. Regions such as FEF, VIP, and MST respond to both visual and vestibular bimodal information and are involved in the integration of multimodal information (Fetsch et al., 2011; Murray & Wallace, 2012). However, due to the inability of brain imaging technologies like MRI to accurately simulate real vestibular stimuli, studies often use alternative stimuli such as electrical stimulation to activate the vestibular organs (Berger et al., 2024; Yang et al., 2024). These alternative stimuli are difficult to control and prone to confounding effects, introducing numerous disruptive factors that complicate the study of the integration mechanisms between visual and vestibular modalities. Single-modal stimuli have many limitations, as changing the magnitude of the conflict may introduce interference from factors like stimulus intensity, which hinders the accurate reflection of the integration mechanisms underlying visual-vestibular conflict.

Numerous studies have reported brain regions associated with susceptibility to motion sickness, including the prefrontal cortex (PFC, IFG), occipital, temporal (MT+), parietal, and central motor regions.

A significant portion of these regions likely contributes to the integration of visual-vestibular self-motion perception (e.g., MT+, parietal, and occipital areas), while some brain regions may also participate in the integration of other forms of sensory information, such as somatosensory (Blume et al., 2022; Jang et al., 2022; Krokos & Varshney, 2022; Li & Zanto, 2024; Liu et al., 2022; Nürnberger et al., 2021; Sakai et al., 2022; Zhu et al., 2024). However, the precise role of these brain regions in mitigating motion sickness remains unclear.

There is relatively limited research on using visual-vestibular bimodal stimulation to study self-motion perception. This study, by employing EEG to measure brain activity, investigates the mechanisms underlying motion sickness and attempts to further explore the brain's response to varying degrees of conflict between visual and vestibular stimuli. An experimental platform combining visual and vestibular stimuli was developed, incorporating an experimental electric wheelchair, wheelchair tracks, and wireless EEG devices. This platform allows for controlled experimental conditions for visual-vestibular stimulation, providing brain activity data under real vestibular stimulation conditions.

METHOD

Participants and Equipment

Six healthy university students (3 males and 3 females, aged 18–22 years) were recruited for the experiment. Participants reported no history of gastrointestinal disorders, cardiovascular diseases, vestibular dysfunction, or alcohol abuse. They also confirmed good sleep quality, no medication use, and normal or corrected-to-normal vision during the experiment. Participants were instructed to remain relaxed throughout the session and wore noise-canceling earplugs to minimize external environmental disturbances.

In this study, EEG signals were recorded using the Neuracle NeuSen W-series 32-channel wireless EEG system during the experimental process (see Figure 1). The experiment was conducted in a quiet, enclosed, and dark room with all unnecessary electronic devices removed to minimize signal interference. A straight wheelchair track approximately 3 meters long was set up in the room, and a remote control was used to maneuver the wheelchair for horizontal back-and-forth movement along the track during the experiment.

To prevent interruptions, EEG signals were continuously recorded throughout the entire experimental process. The EEG recorder was set to a sampling frequency of 1000 Hz. To ensure signal quality, the conductive gel was applied between the EEG electrodes and the participants' scalp, reducing the impedance of all channels to below 10 kΩ.

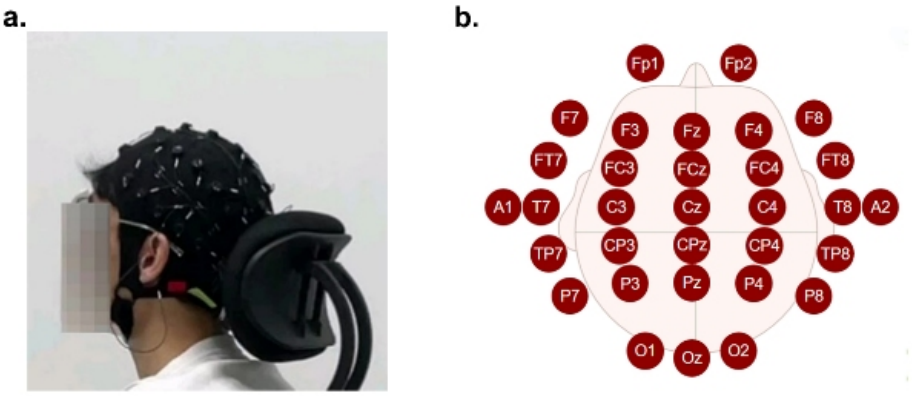

Figure 1: Participant equipped with EEG cap (a) and electrode positions (b).

Experimental Protocol

Before the experiment, participants were instructed to clean their scalps to reduce interference from natural oils that might affect EEG signal acquisition. Following this, participants were assisted in wearing the EEG recorder and seated securely in the motorized wheelchair, ensuring stability to minimize movement artifacts.

The experiment consisted of three conditions: *Condition one*: Conducted in a dark room, participants kept their eyes open throughout the session. *Condition two*: Conducted in a bright room, participants kept their eyes open while wearing a translucent, non-visual eye mask that allowed them to perceive brightness without visualizing objects. *Condition three*: Conducted in a bright room, participants kept their eyes open and were instructed to continuously focus on a fixation point on the wall.

During all three conditions, participants were not required to respond actively, and their EEG signals were recorded continuously.

The experimental procedure for each trial was as follows:

Upon hearing an auditory cue (300 ms), the experimenter maneuvered the wheelchair forward for 8 seconds. A second auditory cue (300 ms) signaled the experimenter to maneuver the wheelchair backward for 12 seconds.

Each trial consisted of one forward and one backward movement. Participants completed 120 trials per condition, with a 5-minute rest provided after every 20 trials. At the end of the experiment, participants filled out a questionnaire.

For *condition two*, the translucent, non-visual eye mask allowed participants to perceive light but prevented them from seeing objects. Participants were required to wear the mask and keep their eyes open throughout the session. In *condition three*, participants maintained continuous focus on a cross-shaped fixation point on the wall (see Figure 2).

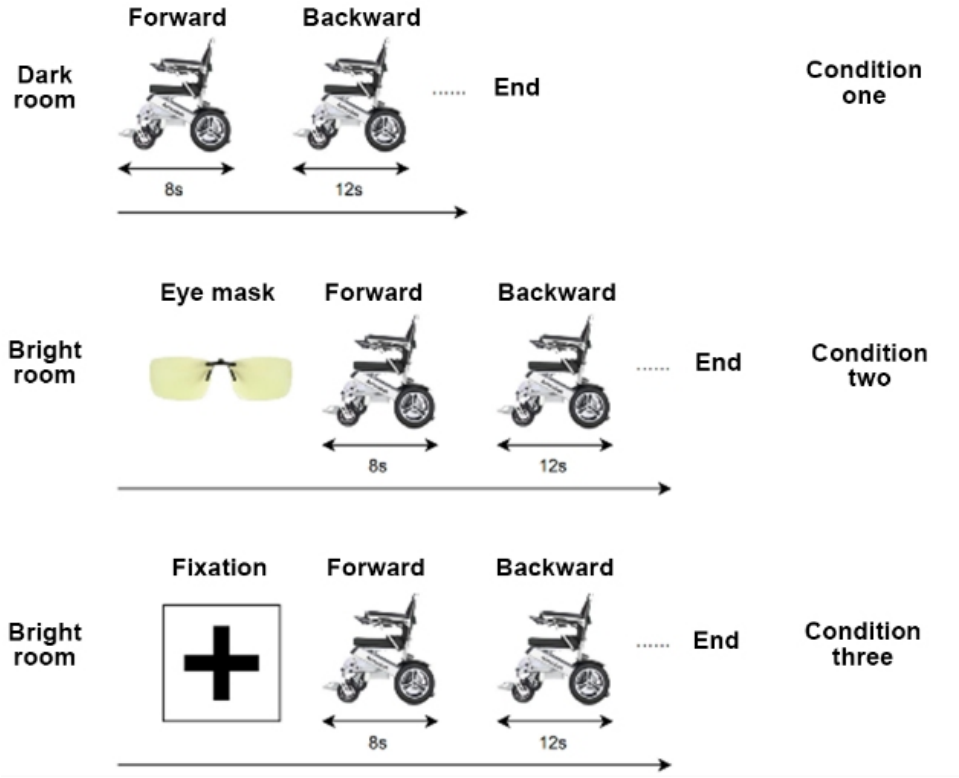

Figure 2: Experimental protocol.

Data Processing

Preprocessing

The raw EEG data contained interference from physiological, instrumental, and environmental sources. Before feature analysis, a 50 Hz notch filter was applied to remove power line noise. EEG spectra were broadly divided into five frequency bands: δ (1–4 Hz), θ (4–8 Hz), α (8–12 Hz), β (12–32 Hz), and γ (32–64 Hz). A band-pass filter of 0.1–32 Hz was used to extract δ to β band power.

Following digital filtering, the EEG data were resampled to 500 Hz to reduce data volume. Eye blinks, a common source of electrooculogram (EOG) artifacts, were addressed using Independent Component Analysis (ICA). The MATLAB-based EEGLAB toolbox was employed to decompose the EEG signals into 32 independent components. Components with an artifact probability exceeding 0.6, such as EOG, electromyogram (EMG), and electrocardiogram (ECG) artifacts, were removed.

Feature Extraction

Fast Fourier Transform (FFT) was used to convert time-domain signals into the frequency domain. The frequency-domain signals were averaged, and the mean values for δ (0.1–4 Hz), θ (4.1–8 Hz), α (8.1–12 Hz), and β (12.1–32 Hz) bands were extracted for each electrode.

Statistical Analysis

Average power across different frequency bands was calculated, and differences between conditions were analyzed.

RESULT

MSSQ and SSQ

The SSQ scale demonstrated high reliability with a Cronbach's α coefficient of 0.972. Since nausea scores under consistent visual information conditions exhibited slight skewness, logarithmic transformation (Ln) was applied. After transformation, the Shapiro-Wilk normality test yielded $P > 0.05$ for all variables, indicating normal distribution.

A single-variable within-subjects design was used to analyze participants' scores across the sub-score of oculomotor, disorientation, and nausea under the three experimental conditions. Repeated-measures ANOVA indicated no significant differences across conditions for any of the sub-scores (see Figure 3).

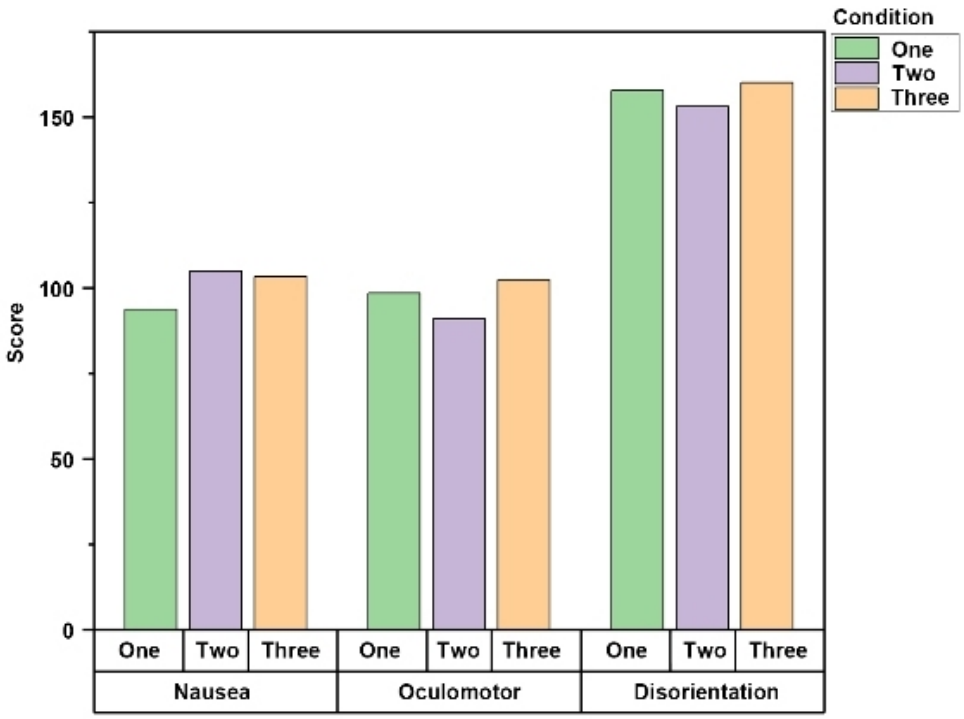

Figure 3: SSQ score of different conditions.

EEG Feature Extraction Results

Significant differences in delta wave (4–8 Hz) power were observed under different movement direction conditions at the FCz, Cz, O1, and O2 channels. Specifically, the delta power at FCz during backward motion was

significantly greater than during forward motion (P = 0.022, F = 13.243, partial η^2 = 0.768). Similarly, at Cz, the backward delta power was significantly higher than the forward condition (P = 0.025, F = 12.250, partial η^2 = 0.754). In contrast, at O1 and O2, forward motion showed significantly greater delta power compared to backward motion (O1: P = 0.022, F = 12.250, partial η^2 = 0.754; O2: P = 0.033, F = 10.286, partial η^2 = 0.720). Additionally, delta power was positively correlated with the degree of visual information conflict (P < 0.05, r = 0.633) (see Figure 4).

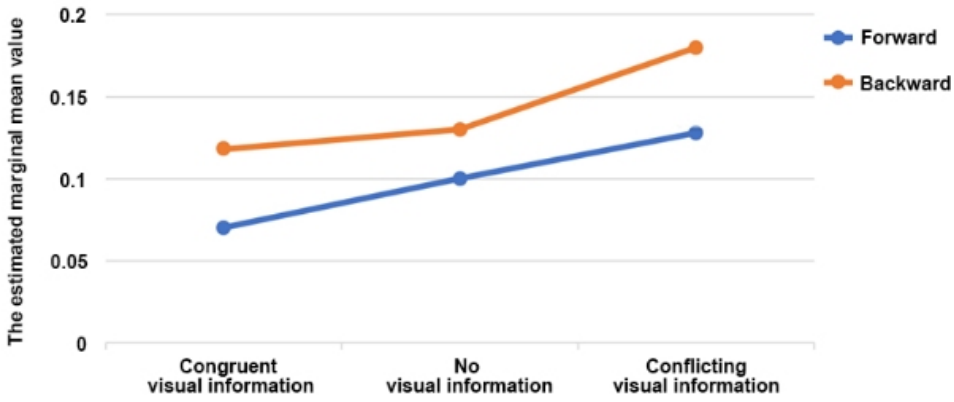

Figure 4: The estimated marginal mean value of the delta wave.

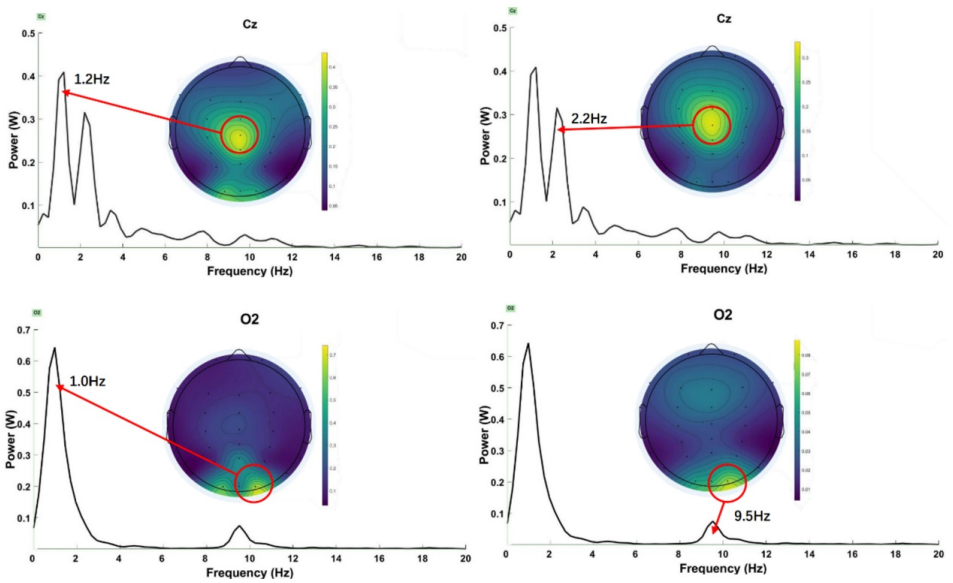

Figure 5: Topographic of absolute energy value and power of channel Cz and O2.

For alpha waves (8–12 Hz), significant differences were found under different movement direction conditions at the O1 and O2 channels. At O1, forward motion elicited significantly greater alpha power than backward motion ($P = 0.045$, $F = 8.340$, partial $\eta^2 = 0.676$). A similar pattern was observed at O2, where forward motion resulted in significantly greater alpha power compared to backward motion ($P = 0.035$, $F = 9.846$, partial $\eta^2 = 0.711$). No significant differences were observed for other frequency bands under movement direction conditions or for any frequency band under motion conflict conditions ($P > 0.05$).

Re-referencing analysis was conducted to calculate the absolute differences in significant frequency bands under different movement direction conditions. The most notable differences were observed in the delta wave at the parietal Cz and occipital O2 channels. At Cz, the delta wave exhibited substantial differences at 1.2 Hz (∼0.4 W) and 2.2 Hz (∼0.3 W). At O2, the delta wave showed a pronounced difference at 1.0 Hz (∼0.65 W), while the alpha wave displayed a notable difference at 9.5 Hz (∼0.1 W) (see Figure 5).

DISCUSSION

Understanding the mechanisms underlying motion sickness has significant practical implications, particularly given its widely accepted association with "sensory conflict"—especially between visual and vestibular inputs. This study aimed to explore EEG characteristics under conditions of visual–vestibular conflict. We examined neural responses to two directions of motion (forward and backward) combined with three types of conflict conditions.

Empirical studies have shown that backward motion tends to induce stronger motion sickness than forward motion (Hartmann et al., 2022; Hughes et al., 2024; Kuiper et al., 2020; Salter et al., 2019)—for instance, passengers sitting backwards in vehicles are more susceptible to discomfort than those facing forward. In this study, we found that delta-band activity was higher during backward motion compared to forward motion. This is consistent with previous findings that delta activity tends to be stronger under conditions that are more likely to induce motion sickness (Woo et al., 2023; Wood et al., 1990; Yeo et al., 2022). Our results extend these findings by providing neural evidence under real physical motion, suggesting that delta activity could serve as a potential indicator of motion sickness severity. This offers valuable insights for future applications, such as predicting individual susceptibility in dynamic travel settings.

Furthermore, delta power was highest under conditions of conflicting visual-vestibular information. Although both subjective reports and EEG measures exhibited only trend-level differences—due to the small sample size—this experimental paradigm holds promise for future research.

Future studies should increase the sample size, refine experimental paradigms, and explore additional EEG features to characterize motion sickness. The feasibility of using spectral features for quantitative evaluation of motion sickness episodes could also be investigated.

ACKNOWLEDGMENT

The authors would like to thank the National Natural Science Foundation of China under project No. 32200923 and Shenzhen Science and Technology Innovation Committee for partially supporting the work via project No. 20220810172237002, No. 20231124100927001.

The authors also would like to thank Qian Sen, Yang Zifeng, Gao Yunfei and Ma Xinyang, who had made great contribution to the experiment and paper.

CONFLICT OF INTEREST

The authors declare that they have no conflict of interest.

REFERENCES

Berger, L. M., Wood, G., & Kober, S. E. (2024). Influence of a placebo tDCS treatment on cybersickness and EEG-neurofeedback success. *Behavioural Brain Research*, *465*, 114917. https://doi.org/10.1016/j.bbr.2024.114917

Blume, M., Schmidt, R., Schmidt, J., Martin, A., & Hilbert, A. (2022). EEG Neurofeedback in the Treatment of Adults with Binge-Eating Disorder: A Randomized Controlled Pilot Study. *Neurotherapeutics*, *19*(1), 352–365. https://doi.org/10.1007/s13311-021-01149-9

Fetsch, C. R., Pouget, A., DeAngelis, G. C., & Angelaki, D. E. (2011). Neural correlates of reliability-based cue weighting during multisensory integration. *Nature Neuroscience*, *15*(1), 146–154. https://doi.org/10.1038/nn.2983

Hartmann, A., Cyberski, C., Schönfeld, U., Krzok, W., & Müller, S. (2022). *Effect of Horizontal Acceleration and Seat Orientation on Motion Sickness in Passenger Cars*.

Henriques, I. F., Douglas de Oliveira, D. W., Oliveira-Ferreira, F., & Andrade, P. M. O. (2014). Motion sickness prevalence in school children. *European Journal of Pediatrics*, *173*(11), 1473–1482. https://doi.org/10.1007/s00431-014-2351-1

Hughes, B. P., Naeem, H. N., & Davidenko, N. (2024). Factors affecting vection and motion sickness in a passive virtual reality driving simulation. *Scientific Reports*, *14*(1), 30214. https://doi.org/10.1038/s41598-024-80778-4

Jang, K.-M., Kwon, M., Nam, S. G., Kim, D., & Lim, H. K. (2022). Estimating objective (EEG) and subjective (SSQ) cybersickness in people with susceptibility to motion sickness. *Applied Ergonomics*, *102*, 103731. https://doi.org/10.1016/j.apergo.2022.103731

Koch, A., Cascorbi, I., Westhofen, M., Dafotakis, M., Klapa, S., & Kuhtz-Buschbeck, J. P. (2018). The Neurophysiology and Treatment of Motion Sickness. *Deutsches Arzteblatt International*, *115*(41), 687–696. https://doi.org/10.3238/arztebl.2018.0687

Krokos, E., & Varshney, A. (2022). Quantifying VR cybersickness using EEG. *Virtual Reality*, *26*(1), 77–89. https://doi.org/10.1007/s10055-021-00517-2

Kuiper, O. X., Bos, J. E., Schmidt, E. A., Diels, C., & Wolter, S. (2020). Knowing What's Coming: Unpredictable Motion Causes More Motion Sickness. *Human Factors*, *62*(8), 1339–1348. https://doi.org/10.1177/0018720819876139

Lackner, J. R. (2014). Motion sickness: More than nausea and vomiting. *Experimental Brain Research*, *232*(8), 2493–2510. Q4. https://doi.org/10.1007/s00221-014-4008-8

Li, G., & Zanto, T. (2024). Reduced VR motion sickness by applying random-phase transcranial alternating current stimulation to the left parietal cortex. *Brain Stimulation*, *17*(3), 550–552. https://doi.org/10.1016/j.brs.2024.04.015

Liu, S., Hao, X., Liu, X., He, Y., Zhang, L., An, X., Song, X., & Ming, D. (2022). Sensorimotor rhythm neurofeedback training relieves anxiety in healthy people. *Cognitive Neurodynamics*, *16*(3), 531–544. https://doi.org/10.1007/s11571-021-09732-8

Murray, M. M., & Wallace, M. T. (Eds.). (2012). *The Neural Bases of Multisensory Processes*. CRC Press/Taylor & Francis. http://www.ncbi.nlm.nih.gov/books/NBK92848/

Nürnberger, M., Klingner, C., Witte, O. W., & Brodoehl, S. (2021). Mismatch of Visual-Vestibular Information in Virtual Reality: Is Motion Sickness Part of the Brains Attempt to Reduce the Prediction Error? *Frontiers in Human Neuroscience*, *15*, 757735. https://doi.org/10.3389/fnhum.2021.757735

Parker, D. E. (1977). [Review of *Review of Motion Sickness*, by J. T. Reason & J. J. Brand]. *The American Journal of Psychology*, *90*(1), 182–188. https://doi.org/10.2307/1421659

Reason, J. T., & Brand, J. J. (1975). *Motion sickness* (pp. vii, 310). Academic Press.

Sakai, H., Harada, T., Larroque, S. K., Demertzi, A., Sugawara, T., Ito, T., Wada, Y., Fukunaga, M., Sadato, N., & Laureys, S. (2022). Left parietal involvement in motion sickness susceptibility revealed by multimodal magnetic resonance imaging. *Human Brain Mapping*, *43*(3), 1103–1111. https://doi.org/10.1002/hbm.25710

Salter, S., Diels, C., Herriotts, P., Kanarachos, S., & Thake, D. (2019). Motion sickness in automated vehicles with forward and rearward facing seating orientations. *Applied Ergonomics*, *78*, 54–61. https://doi.org/10.1016/j.apergo.2019.02.001

Schmäl, F. (2013). Neuronal Mechanisms and the Treatment of Motion Sickness. *Pharmacology*, *91*(3–4), 229–241. Q3. https://doi.org/10.1159/000350185

Tian, N., Lopes, P., & Boulic, R. (2022). A review of cybersickness in head-mounted displays: Raising attention to individual susceptibility. *Virtual Reality*, *26*(4), 1409–1441. https://doi.org/10.1007/s10055-022-00638-2

Wei, Y., Wang, Y., Okazaki, Y. O., Kitajo, K., & So, R. H. Y. (2024). Motion sickness resistant people showed suppressed steady-state visually evoked potential (SSVEP) under vection-inducing stimulation. *Cognitive Neurodynamics*, *18*(4), 1525–1537. https://doi.org/10.1007/s11571-023-09991-7

Woo, Y. S., Jang, K.-M., Nam, S. G., Kwon, M., & Lim, H. K. (2023). Recovery time from VR sickness due to susceptibility: Objective and quantitative evaluation using electroencephalography. *Heliyon*, *9*(4), e14792. https://doi.org/10.1016/j.heliyon.2023.e14792

Wood, C. D., Stewart, J. J., Wood, M. J., Manno, J. E., Manno, B. R., & Mims, M. E. (1990). Therapeutic effects of antimotion sickness medications on the secondary symptoms of motion sickness. *Aviation, Space, and Environmental Medicine*, *61*(2), 157–161.

Yang, M., Li, Z., Pan, F., Wu, S., Jia, X., Wang, R., Ji, L., Li, W., & Li, C. (2024). Alpha tACS on Parieto-Occipital Cortex Mitigates Motion Sickness Based on Multiple Physiological Observation. *IEEE Transactions on Neural Systems and Rehabilitation Engineering*, *32*, 2398–2407. IEEE Transactions on Neural Systems and Rehabilitation Engineering. https://doi.org/10.1109/TNSRE.2024.3419753

Yates, B. J., Catanzaro, M. F., Miller, D. J., & McCall, A. A. (2014). Integration of vestibular and emetic gastrointestinal signals that produce nausea and vomiting: Potential contributions to motion sickness. *Experimental Brain Research*, *232*(8), 2455–2469. https://doi.org/10.1007/s00221-014-3937-6

Yeo, S. S., Kwon, J. W., & Park, S. Y. (2022). EEG-based analysis of various sensory stimulation effects to reduce visually induced motion sickness in virtual reality. *Scientific Reports*, *12*(1), 18043. https://doi.org/10.1038/s41598-022-21307-z

Zhang, L.-L., Wang, J.-Q., Qi, R.-R., Pan, L.-L., Li, M., & Cai, Y.-L. (2016). Motion Sickness: Current Knowledge and Recent Advance. *CNS Neuroscience & Therapeutics*, *22*(1), 15–24. https://doi.org/10.1111/cns.12468

Zhu, J., Bao, X., Huang, Q., Wang, T., Huang, L., Han, Y., Huang, H., Zhu, J., Qu, J., Li, K., Chen, D., Jiang, Y., Xu, K., Wang, Z., Wu, W., & Li, Y. (2024). *A Wearable Mindfulness Brain–Computer Interface for Alleviating Car Sickness* (p. 2024.09.25.614936). bioRxiv. https://doi.org/10.1101/2024.09.25.614936